THE JOURNAL OF PHYSICAL CHEMISTRY C

ARTICLE

pubs.acs.org/JPCC

Interactions of Silica Nanoparticles and Ionic Liquids Probed by High Pressure Vibrational Spectroscopy

Hai-Chou Chang,*[,†] Tzu-Chieh Hung,[†] Shu-Chieh Chang,[†] Jyh-Chiang Jiang,[‡] and Sheng Hsien Lin[§,∥]

[†]Department of Chemistry, National Dong Hwa University, Shoufeng, Hualien 974, Taiwan

[‡]Department of Chemical Engineering, National Taiwan University of Science and Technology, Taipei 106, Taiwan

[§]Department of Applied Chemistry, National Chiao Tung University, Hsinchu 30010, Taiwan

[∥]Institute of Atomic and Molecular Sciences, Academia Sinica, P.O. Box 23-166, Taipei 106, Taiwan

Supporting Information

ABSTRACT: Gel-like ionic liquid/nanosilica mixtures have been prepared with the addition of 10 wt % nanosilica to 1-ethyl-3-methylimidazolium bis(trifluoromethylsulfonyl)amide (EMI^+-$TFSA^-$), but no changes in C−H spectral features of EMI^+TFSA^- were observed in the presence of nanosilica under ambient pressure. As the gel-like mixture of EMI^+TFSA^-/nanosilica was compressed, a new alkyl C−H band at ca. 3017 cm^{-1} arose. This new spectral feature at ca. 3017 cm^{-1} may be attributed to the structural reorganization of alkyl C−H groups induced by the interactions between ionic clusters and nanosilica. The imidazolium C−H bands display nonmonotonic shifts as the pressure is elevated. They blue shift slightly initially, but red shifts occur upon further increase of the pressure. The compression also leads to an increase in the relative intensity of the imidazolium C−H band at ca. 3105 cm^{-1}. This observation suggests that some associated species are switched to the isolated form due to the presence of nanosilica under high pressures. In contrast to EMI^+TFSA^-/nanosilica, the band frequencies and band shapes of 1-butyl-3-methylimidazolium bis(trifluoromethylsulfonyl)amide (BMI^+TFSA^-)/nanosilica are similar to those of pure BMI^+TFSA^-. These results indicate that the length of alkyl C−H groups plays a nonnegligible role in isolated-associated equilibrium.

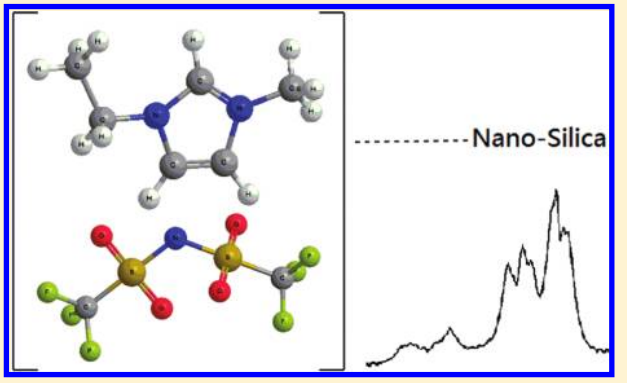

INTRODUCTION

The excellent properties of ionic liquids, such as very low vapor pressures and wide temperature ranges of liquid phase, have attracted the attention of a large number of researchers in many fields.[1−3] One of the promised applications of ionic liquids is the potential to be ideal nonvolatile solvents, making them replacements for volatile organic solvents.[1−3] Ionic liquids are understood as liquids consisting entirely of ions and having melting points below 100 °C. Typically ionic liquids are built up by a bulky, asymmetric organic cation to prevent ions from packing easily. This asymmetry opposes strong charge ordering due to the ionic interactions, and thus, the melting points of ionic liquids may be below or near room temperature. Since ionic liquids are composed of ions, their characteristics can be tuned by changing the anions, cations, and attached substituents.[1−5] For example, ionic liquids could be designed to be made hydrophobic by choice of anion species.[1] Although the literature contains many articles on the application of ionic liquids as solvents, studies on the phase behavior of ionic liquids in the presence of nanoparticles are scarce. In this study, we mixed ionic liquids with silica nanoparticles to prepare gel-like mixtures and used variable pressure as a window to look into the nature of local geometric properties.

The ordering of ionic liquids at solid surfaces is a subject of recent intense research activities.[6−18] As ionic liquids are composed solely of ions, their bulk behavior is mainly governed by Coulombic forces. Ionic liquids differ from the classical salts at least in one aspect: they possess hydrogen bonds that induce structural directions. For the ionic liquid/solid interface, the structural rearrangement of the cations and anions was observed.[11−17] Microscopic structures of solid−ionic liquid interfaces on various surfaces, such as gold,[13] mica,[14] sapphire,[15] graphite,[16] platinum,[17] and SiO_2,[11] have been studied in detail by experiments and theoretical simulation. Based on these studies, solvation layers are found at the solid−ionic liquid interfaces for various ionic liquids and the strength of the interaction between the innermost solvation layer and the substrate is dependent on the cation type.[11−17]

In recent years, ionic liquids based on 1-alkyl-3-methylimidazolium cation have received much attention. One of the attractive features of the 1-alkyl-3-methylimidazolium cation is the

Received: March 23, 2011
Revised: May 13, 2011
Published: May 20, 2011

inherently amphiphilic character as a surfactant. Both experiments and theoretical studies found that ionic liquids may not be regarded as homogeneous solvents but must be considered as nanostructured with polar and nonpolar regions.[19−21] In other words, ionic liquids can display remarkable structural heterogeneity. Research on ionic liquids has found that the alkyl side chain length has an influence on the supramolecular assemblies of ionic liquids.[22] Aggregation effects between alkyl tails can lead to ordered local environment, even for alkyl chains as short as butyl.[22] In the present study, our intent is to achieve further understanding of the effect of alkyl side chain length in ionic liquid/nanosilica mixtures.

Ionic liquid based mixtures have received a lot of attention in recent years.[23−26] Much of this research is interested in the interactions of anions. For example, the presence of anion−water interactions has profound effects on the physical properties of ionic liquids. Water molecules seem to be separated from each other at low content, while self-association appears at higher concentration. At high ionic liquid concentration, ionic liquids form clusters as in the pure state and water molecules interact with the clusters without interacting among themselves.[27,28] The hydrogen bonding interactions are complex for ionic liquid based mixtures with varying anions, due to pronounced anionic interactions. In contrast to anionic interactions, the study of the cationic interactions has been limited.[27−31] In this work, we demonstrate that cation−nanosilica interactions play a nonnegligible role in ionic liquid/nanosilica mixtures.

Various studies have been performed to elucidate the role of weak hydrogen bonds, such as C−H···O and C−H···X, in the structure of ionic liquids.[1−4] For the 1-alkyl-3-methylimidazolium-type ionic liquids, the strongest hydrogen bond involves the most acidic C^2−H of the imidazolium cation, followed by C^4−H and C^5−H. One of the intriguing aspects of weak hydrogen bonds is that the C−H covalent bond tends to shorten as a result of formation of a hydrogen bond. Scheiner's group[32,33] and Dannenberg's group[34] view conventional and C−H···O hydrogen bonds to be very similar in nature. The origin of both the red- and blue-shifted hydrogen bonds was also concluded to be the same by the Schlegel group[35] and the Hermansson group.[36]

The development of diamond anvil cells has opened up possibilities for spectroscopic experiments at high pressures. In this article, we present the results of a quantitative in situ infrared spectroscopic study at pressures from 0.1 MPa to 2.5 GPa.[27−31] Such pressures mainly change intermolecular distances and affect conformations. Under high pressures, the relative weights of the intermolecular forces defining the aggregation state are altered, and the repulsive side of the intermolecular potential is explored.[27−31,37] Studies have shown the significant effect that pressure has on probing the microscopic structures of pure ionic liquids and ionic liquid based mixtures.[27−31] In this study, we show that high pressure is a sensitive method to probe ionic-association structures of ionic liquids in the presence of nanosilica.

EXPERIMENTAL SECTION

Samples were prepared using 1-ethyl-3-methylimidazolium bis(trifluoromethylsulfonyl)amide (>97%, Fluka), 1-butyl-3-methylimidazolium bis(trifluoromethylsulfonyl)amide (>98%, Fluka), and silicon dioxide nanopowder (10−20 nm, 99.5%, Aldrich). A diamond anvil cell (DAC) of Merril−Bassett design, having a diamond culet size of 0.6 mm, was used for generating pressures up to ca. 2 GPa. Two type IIa diamonds were used for mid-infrared measurements. The sample was contained in a 0.3-mm-diameter hole in a 0.25-mm-thick Inconel gasket mounted on the diamond anvil cell. To reduce the absorbance of the samples, CaF_2 crystals (prepared from a CaF_2 optical window) were placed into the hole and compressed firmly prior to insertion of the sample. A droplet of a sample filled the empty space of the entire hole of the gasket in the DAC, which was subsequently sealed when the opposed anvils were pushed toward one another. Infrared spectra of the samples were measured on a Perkin-Elmer Fourier transform spectrophotometer (Model Spectrum RXI) equipped with a LITA (lithium tantalite) mid-infrared detector. The infrared beam was condensed through a 5X beam condenser onto the sample in the diamond anvil cell. Typically, we chose a resolution of 4 cm^{-1} (data point resolution of 2 cm^{-1}). For each spectrum, typically 1000 scans were compiled. To remove the absorption of the diamond anvils, the absorption spectra of DAC were measured first and subtracted from those of the samples. Pressure calibration followed Wong's method.[38,39] The pressure dependence of screw moving distances was measured.

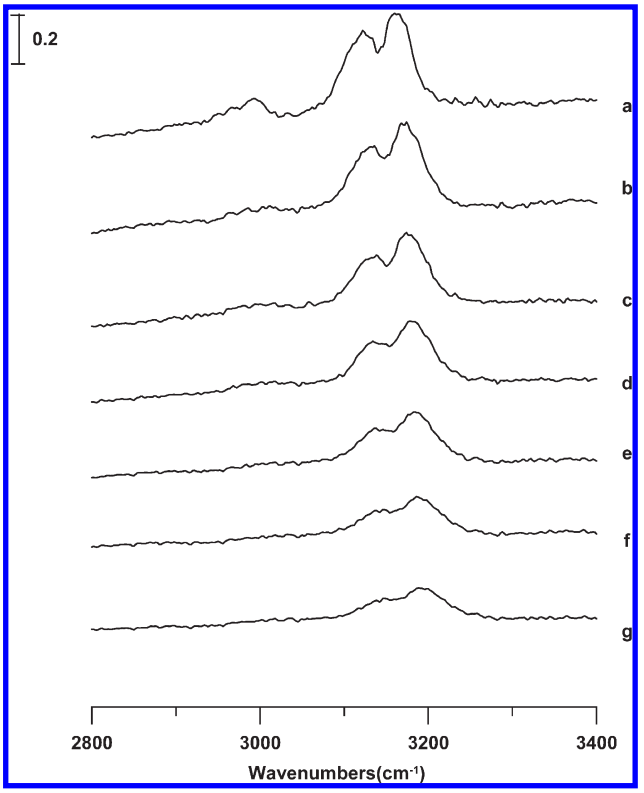

Figure 1. IR spectra of an EMI^+TFSA^-/nanosilica mixture (2 wt % nanosilica) obtained under ambient pressure (a) and at 0.3 (b), 0.9 (c), 1.5 (d), 1.9 (e), 2.3 (f), and 2.5 GPa (g).

RESULTS AND DISCUSSION

Figure 1 displays infrared spectra of an 1-ethyl-3-methylimidazolium bis(trifluoromethylsulfonyl)amide (EMI^+TFSA^-)/nanosilica mixture having nanosilica equal to 2 wt % obtained under ambient pressure (Figure 1a) and at 0.3 (Figure 1b), 0.9 (Figure 1c), 1.5 (Figure 1d), 1.9 (Figure 1e), 2.3 (Figure 1f), and 2.5 GPa (Figure 1g). The bis(trifluoromethylsulfonyl)amide anion $(CF_3SO_2)_2N^-$ is also called NTf_2^-, Tf_2N^-, and $TFSI^-$ in the literature. As revealed in Figure 1a, the peaks at 3123 and

3162 cm^{-1} can be attributed to coupled imidazolium C−H stretching modes of C^2−H, C^4−H, and C^5−H.[27−31] A weak shoulder at 3103 cm^{-1} is also observed in Figure 1a.[40] In comparison to the spectrum of pure EMI^+TFSA^-,[31] we observe no drastic changes of the C−H bands in the presence of nanosilica in Figure 1a. The nearly degenerated peaks, i.e., 3103 and 3123 cm^{-1}, indicate the perturbation of neighboring ions in the liquid state.[40] The imidazolium C−H may exist at least in two different forms, i.e., isolated and associated structures. On the basis of previous concentration-dependent results, the spectral feature at approximately 3103 cm^{-1} should be assigned to the isolated (or dissociated) structure.[30,31] The associated species may be larger ion clusters (or ion pairs), and the isolated species may mean the dissociation into smaller ion clusters (or free ions). The splitting of the nearly degenerated bands was assigned by Ludwig's group to the existence in the bulk phase of isolated pairs with stronger hydrogen bonding to the counteranion, in addition to associated ion pairs with weaker hydrogen bonding.[40] As the sample was compressed to 0.3 GPa (Figure 1b), the two major imidazolium C−H bands were blue shifted to 3132 and 3173 cm^{-1}, respectively. As the sample was further compressed, i.e., increasing the pressure from 0.3 (Figure 1b) to 0.9 GPa (Figure 1c), pressure-induced frequency shifts of the imidazolium C−H bands were relatively small, as shown in Figure 1b,c. As shown in Figure 1d−g, the compression leads to further blue shifts in frequency.

Although gelation does not occur with the addition of 2 wt % nanosilica to EMI^+TFSA^-, gelation can be observed with the addition of 10 wt % nanosilica.[6] The 10 wt % mixture was highly viscous and did not drop when the centrifuge capsule was turned upside down. Figure 2 shows infrared spectra of an EMI^+TFSA^-/nanosilica mixture having nanosilica equal to 10 wt % obtained under ambient pressure (Figure 2a) and at 0.3 (Figure 2b), 0.9 (Figure 2c), 1.5 (Figure 2d), 1.9 (Figure 2e), 2.3 (Figure 2f), and 2.5 GPa (Figure 2g). By comparing Figure 1a with Figure 2a, we found that the presence of 10 wt % nanosilica has a negligible effect on the spectral features of C−H stretching bands under ambient pressure in Figure 2a. This observation may suggest that the infrared measurement may not be a sensitive enough tool to monitor the transition of gelation under ambient pressure. It is instructive to note that the gelation occurs at ionic liquid rich concentrations, i.e., 10 wt % nanosilica, in Figure 2. Studies of SiO_2-rich mixtures have shown that the interaction between SiO_2 and ionic liquids produces red shifts in frequencies for imidazolium C−H vibrations.[8] Theoretical calculations also indicate that SiO_2 prefers to interact more with the imidazolium C−H groups than with alkyl C−H groups at ambient pressure.[8] As the gel-like mixture was compressed, i.e., increasing from ambient (Figure 2a) to 0.3 GPa (Figure 2b) and 0.9 GPa (Figure 2c), the blue shifts in frequency were observed for alkyl C−H stretching modes. A further increase in pressure leads to dramatic spectral changes in Figure 2d, as a new alkyl C−H band at 3017 cm^{-1} arose and two major imidazolium C−H bands were red shifted to 3113 and 3159 cm^{-1}, respectively. We notice that no more vibration modes exist in this region (ca. 3107 cm^{-1}), so this new spectral feature located at 3017 cm^{-1} in Figure 2d should be assumed to arise from the structural reorganization of alkyl C−H groups induced by the interactions between ionic clusters and nanosilica. It is well-known that C−H covalent bond tends to shorten as a result of the formation of weak hydrogen bonds.[32−35] This observation suggests the formation of certain C−H···silica or C−H···O interactions around the alkyl C−H groups, but the details remain unclear. As indicated in Figure 2a−c, the infrared spectra of EMI^+TFSA^-/nanosilica are similar to that of pure EMI^+TFSA^- in our previous study[31] up to 0.9 GPa from ambient. The interactions in EMI^+TFSA^-/nanosilica mixtures involve ionic liquid−ionic liquid and ionic liquid−nanosilica interactions. The ionic liquid−nanosilica interactions may not play a dominant role in the mixture with 10 wt % nanosilica under relative low pressures (<0.9 GPa). The observation in Figure 2d may indicate a pressure-induced phase transition caused by pressure-enhanced C−H···O interactions. The sensitivity to changes in pressures may arise from changes in the geometric properties of the hydrogen-bond network. It is interesting to note that the imidazolium C−H bands display nonmonotonic shifts in frequency as the sample was compressed in Figure 2a−d. They blue shift slightly (or show almost no change) in frequency initially in Figure 2a−c, but red shifts occur upon further increasing the pressure in Figure 2c,d. This result is remarkably different from that revealed for alkyl C−H bands in Figure 2a−d. From the point of view of fundamental studies, the nature of weak hydrogen bonds continues to be an important subject. When a molecule that is capable of forming blue-shifting hydrogen bonds binds to a site with a sufficiently strong electrostatic field to dominate over the overlap effect, that molecule is predicted to display a red-shifting hydrogen bond; experimental evidence is still lacking, however.[34] In this study, we present a means of looking at this issue by employing the high-pressure method. The spectral features of the imidazolium C−H stretching

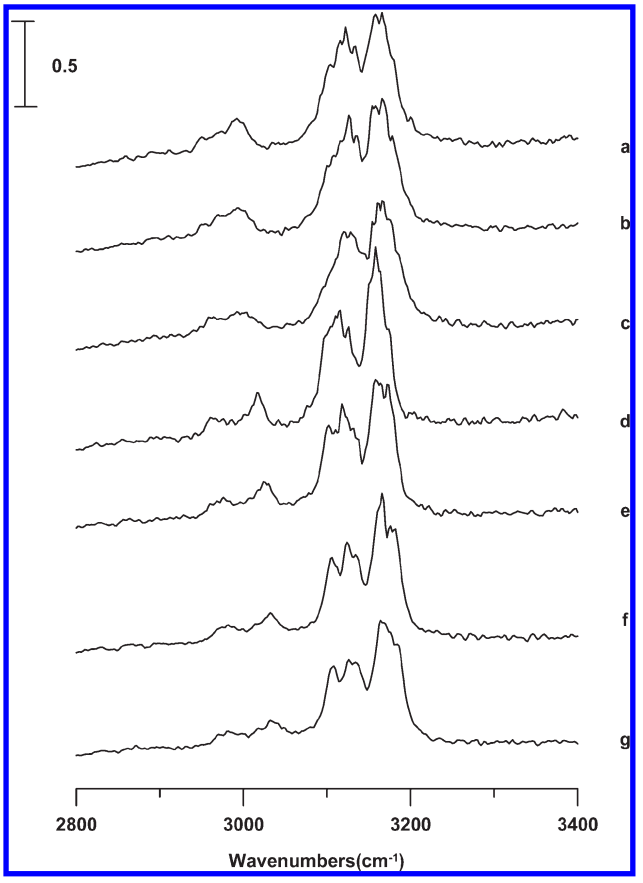

Figure 2. IR spectra of an EMI^+TFSA^-/nanosilica mixture (10 wt % nanosilica) obtained under ambient pressure (a) and at 0.3 (b), 0.9 (c), 1.5 (d), 1.9 (e), 2.3 (f), and 2.5 GPa (g).

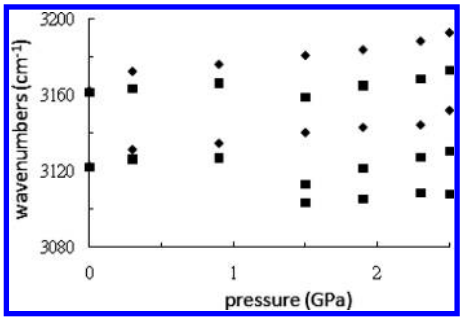

Figure 3. Pressure dependence of the imidazolium C−H stretching frequencies of EMI^+TFSA^-/nanosilica mixtures with 2 wt % nanosilica (diamonds) and 10 wt % nanosilica (squares).

modes showed further evolution upon further compression, as changes in the relative intensities of the imidazolium C−H bands occur in Figure 2e−g. The imidazolium C−H stretching absorption shows four peaks under high pressure in Figure 2e−g. We note that the spectral feature at approximately 3105 cm^{-1} is more pronounced in Figure 2e−g. It is well-known that the absorption band at ca. 3105 cm^{-1} should be attributed to the isolated structures. That is, the compression leads to the increase in the relative intensities of the isolated C−H bands in Figure 2e−g. This observation may suggest that some associated species are switched to the isolated form due to the presence of nanosilica under the condition of high pressures.

Figure 3 illustrates the band frequency of the dominant imidazolium C−H absorption versus the pressure applied. Looking into detail in Figure 3, we observe no significant differences in the weight percent dependence, i.e., 2 and 10 wt %, of the imidazolium C−H band frequencies at lower pressures, i.e., pressure < 1 GPa. Nevertheless, remarkable red shifts and band splitting were observed for the mixture with 10 wt % nanosilica at pressure > 1 GPa. This behavior indicates that the clustering of ionic liquids is perturbed by the presence of nanosilica at high weight percent, i.e., 10 wt % nanosilica, and suggests the formation of certain ionic liquid structures around nanosilica under high pressures. A possible explanation for this effect is the pressure-enhanced C−H···O interactions between alkyl C−H/imidazolium C−H and nanosilica. The pressure-enhanced weak hydrogen bond may be one of reasons for the remarkable transition of EMI^+TFSA^- microstructures from associated clustering to dissociated structures as shown in Figure 2 e−g. In other words, nanosilica can be added to change the hydrogen-bonded network of EMI^+TFSA^- as the pressure is elevated. We note that sufficient amounts (for example 10 wt %) of nanosilica are required to induce the changes in aggregation behaviors of EMI^+TFSA^- as shown in Figures 2 and 3. It is known that cohesion in ionic liquids is strong and mostly electrostatic.[1−3] Nevertheless, this study elucidates the nonnegligible role of C−H hydrogen bonds in the structure of ionic liquids. The energetically favored approach for nanosilica to interact with the EMI^+ cation may be through the formation of imidazolium C−H···O and alkyl C−H···O interactions, whereas the former may play more important roles due to the well-known acidity of imidazolium C−H groups. The oxygen atoms may originate from silica and some absorbed water molecules.

To develop further insight into the associated−dissociated mechanism and the alkyl chain length dependence of the cations, the pressure study of 1-butyl-3-methylimidazolium bis-(trifluoromethylsulfonyl)amide (BMI^+TFSA^-) seems to offer

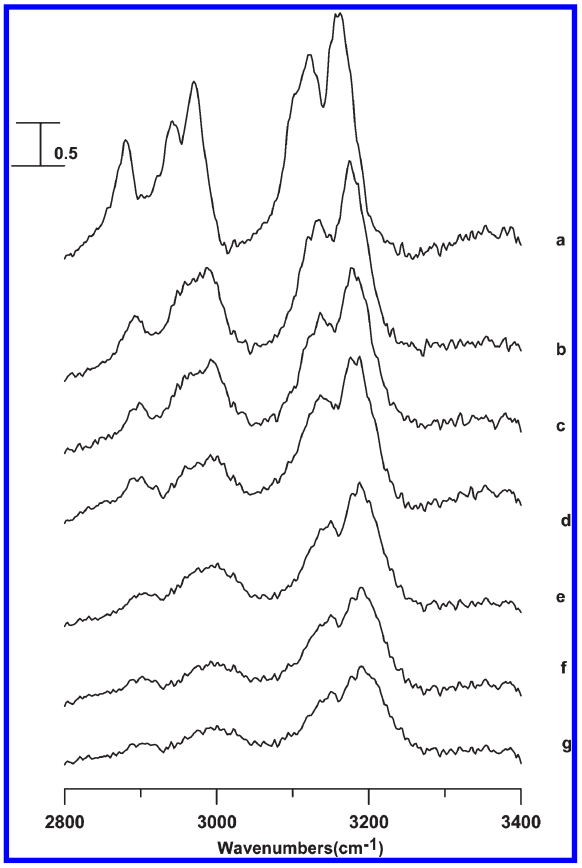

Figure 4. IR spectra of pure BMI^+TFSA^- obtained under ambient pressure (a) and at 0.3 (b), 0.9 (c), 1.5 (d), 1.9 (e), 2.3 (f), and 2.5 GPa (g).

the direct approach. Figure 4 displays infrared spectra of pure BMI^+TFSA^- obtained under ambient pressure (Figure 4a) and at 0.3 (Figure 4b), 0.9 (Figure 4c), 1.5 (Figure 4d), 1.9 (Figure 4e), 2.3 (Figure 4f), and 2.5 GPa (Figure 4g). As shown in Figure 4a, the absorption bands at 2881, 2943, and 2969 cm^{-1} can be attributed to C−H stretching modes of the alkyl groups. It is likely that these infrared bands consist of multiple vibrations, although no attempt was made to deconvolute them. The coupled imidazolium C−H bands locate at 3120 and 3160 cm^{-1}. The appearance of a weak shoulder at approximately 3102 cm^{-1} indicates that the imidazolium C−H may exist at least in two different forms, i.e., associated and isolated forms. As the pressure was elevated, the alkyl and imidazolium C−H bands were blue shifted in Figure 4.

Figure 5 shows infrared spectra of a BMI^+TFSA^-/nanosilica mixture having nanosilica equal to 13 wt % obtained under ambient pressure (Figure 5a) and at 0.3 (Figure 5b), 0.9 (Figure 5c), 1.5 (Figure 5d), 1.9 (Figure 5e), 2.3 (Figure 5f), and 2.5 GPa (Figure 5g). As revealed in Figure 5a, no drastic changes in the presence of nanosilica are observed under ambient pressure. The spectra features of the C−H stretching modes show further evolution upon compression through the observation of blue shifts in frequency in Figure 5b−g. Nevertheless, we do not observe experimental evidence of the appearance of the new alkyl C−H band at ca. 3017 cm^{-1} and the band splitting of the imidazolium C−H bands in Figure 5b−g as revealed for the EMI^+TFSA^-/nanosilica mixture in Figure 2. Figure 6 illustrates the pressure dependence of the band frequency of the dominant imidazolium C−H stretching absorption. Looking into more

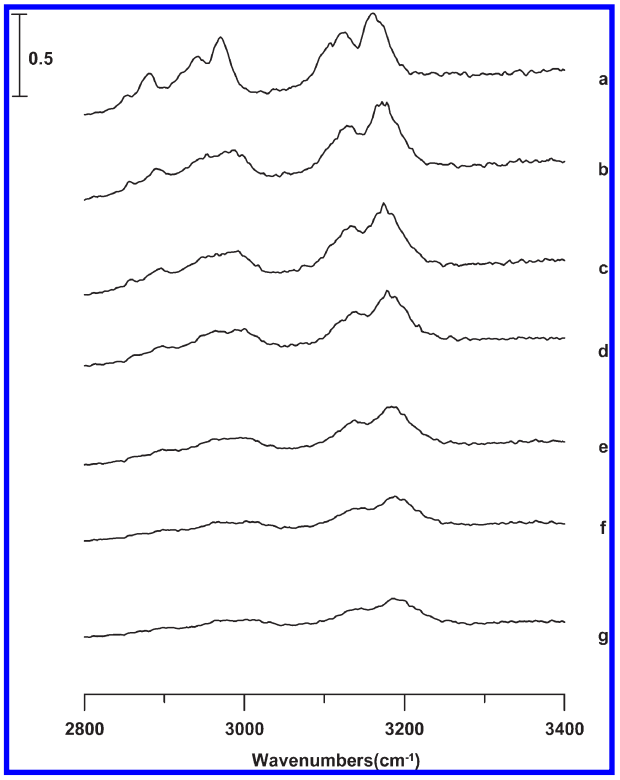

Figure 5. IR spectra of an BMI^+TFSA^-/nanosilica mixture (13 wt % nanosilica) obtained under ambient pressure (a) and at 0.3 (b), 0.9 (c), 1.5 (d), 1.9 (e), 2.3 (f), and 2.5 GPa (g).

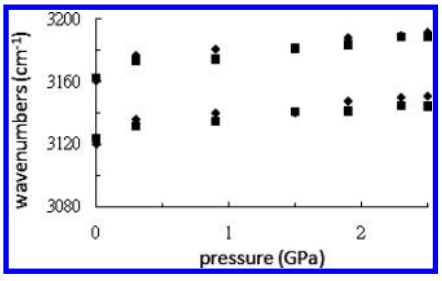

Figure 6. Pressure dependence of imidazolium C−H stretching frequencies of pure BMI^+TFSA^- (diamonds) and a BMI^+TFSA^-/nanosilica mixture with 13 wt % nanosilica (squares).

details in Figure 6, we see that the band frequencies of the BMI^+TFSA^-/nanosilica mixture are almost identical to those of pure BMI^+TFSA^-. These results are remarkably different from what is revealed for imidazolium C−H groups of the EMI^+TFSA^-/nanosilica mixture in Figure 3 and lead us to suggest that the increase in the alkyl chain length may reduce the effects of alkyl C−H···nanosilica interactions under high pressures. That is, the decrease in the alkyl chain length may significant disturb the isolated−associated equilibrium in ionic liquid/nanosilica mixtures. These results suggest that the interactions between imidazolium C−H groups and nanosilica may not be the sole factor to perturb the geometric properties in ionic liquid/nanosilica mixtures, while the alkyl C−H groups may also play nonnegligible roles in isolated−associated equilibrium.

It is known that the imidazolium C−H stretching region may be described by two doublets (four bands): one doublet at the lower frequencies is assigned to the C^2−H stretching modes and another doublet at the higher frequencies is attributed to the coupled C^4−H and C^5−H stretching modes.[40] As shown by Figures S1 and S2 (see the Supporting Information), where frequencies of two doublets have been plotted versus the pressure applied, we see that the spectral perturbation caused by the presence of nanosilica is more pronounced for the EMI^+TFSA^-/nanosilica mixture (Figure S1 in the Supporting Information) than for the BMI^+TFSA^-/nanosilica (Figure S2 in the Supporting Information). This behavior is in accord with the results in Figures 3 and 6 indicating the same trends for imidazolium C−H bands. The way of fitting with four bands, i.e., Figures S1 and S2 in the Supporting Information, does provide more insightful information, but some concerns arise due to the increase in the number of fitting parameters. Suffered by the noise in pressure-dependent data, the deconvoluted bandwidths and relative intensities may not be accurate enough to provide further details (data not shown).

CONCLUSION

We demonstrate that the hydrogen-bond network in ionic liquid/nanosilica mixtures can be probed by high pressure infrared techniques. Perturbation of EMI^+TFSA^- hydrogen-bond structures caused by nanosilica was observed under the condition of high pressures. A new alkyl C−H band appears at ca. 3017 cm^{-1}, originating from the structural reorganization of alkyl C−H groups induced by the interactions between ionic clusters and nanosilica. The imidazolium C−H absorption of EMI^+TFSA^-/nanosilica displays nonmonotonic frequency shifts and band splitting. The spectral feature at ca. 3105 cm^{-1} is more pronounced under high pressures. This observation indicates that some associated species are switched to the isolated forms. It is known that cohesion in ionic liquids is strong and mostly electrostatic. Nevertheless, this study elucidates the nonnegligible role of C−H hydrogen bonds in the local structures of ionic liquid/nanosilica mixtures. The band frequencies of the BMI^+TFSA^-/nanosilica are almost identical to those of pure BMI^+TFSA^-. In other words, the alkyl chain also plays a role in the local structural organization in ionic liquid/nanosilica mixtures.

ASSOCIATED CONTENT

Supporting Information. Pressure dependence of the imidazolium C−H stretching frequencies of EMI^+TFSA^-/nanosilica mixtures with 2 wt % nanosilica and 10 wt % nanosilica (Figure S1) and pressure dependence of the imidazolium C−H stretching frequencies of pure BMI^+TFSA^- and a BMI^+TFSA^-/nanosilica mixture with 13 wt % nanosilica (Figure S2). This material is available free of charge via the Internet at http://pubs.acs.org.

AUTHOR INFORMATION

Corresponding Author

*E-mail: hcchang@mail.ndhu.edu.tw. Fax: +886-3-8633570. Phone: +886-3-8633585.

ACKNOWLEDGMENT

The authors thank the National Dong Hwa University and the National Science Council (Contract No. NSC 98-2113-M-259-005-MY3) of Taiwan for financial support. The authors thank Chen-Pin Duang for his assistance.

REFERENCES

(1) *Ionic Liquids in Synthesis*; Wasserscheid, P., Welton, T., Eds.; Wiley VCH: Weinheim, Germany, 2008.
(2) Castner, E. W.; Wishart, J. F. *J. Chem. Phys.* **2010**, *132*, 120901.
(3) Weingartner, H. *Angew. Chem., Int. Ed.* **2008**, *47*, 654.
(4) Wulf, A.; Fumino, K.; Ludwig, R. *Angew. Chem., Int. Ed.* **2010**, *49*, 449.
(5) Gao, Y.; Zhang, L.; Wang, Y.; Li, H. *J. Phys. Chem. B* **2010**, *114*, 2828.
(6) Ueno, K.; Hata, K.; Katakabe, T.; Kondoh, M.; Watanabe, M. *J. Phys. Chem. B* **2008**, *112*, 9013.
(7) Gobel, R.; Hesemann, P.; Weber, J.; Moller, E.; Friedrich, A.; Beuermann, S.; Taubert, A. *Phys. Chem. Chem. Phys.* **2009**, *11*, 3653.
(8) Singh, M. P.; Singh, R. K.; Chandra, S. *ChemPhysChem* **2010**, *11*, 2036.
(9) Liu, Y.; Wu, G.; Fu, H.; Jiang, Z.; Chen, S.; Sha, M. *Dalton Trans.* **2010**, *39*, 3190.
(10) Zhang, J.; Zhang, Q.; Li, X.; Liu, S.; Ma, Y.; Shi, F.; Deng, Y. *Phys. Chem. Chem. Phys.* **2010**, *12*, 1971.
(11) Rollins, J. B.; Fitchett, B. D.; Conboy, J. C. *J. Phys. Chem. B* **2007**, *111*, 4990.
(12) Sobota, M.; Schmid, M.; Happel, M.; Amende, M.; Maier, F.; Steinruck, H.; Paape, N.; Wasserscheid, P.; Laurin, M.; Gottfried, J. M.; Libuda, J. *Phys. Chem. Chem. Phys.* **2010**, *12*, 10610.
(13) Atkin, R.; Abedin, S. Z. E.; Hayes, R.; Gasparotto, L. H. S.; Borisenko, N.; Endres, F. *J. Phys. Chem. C* **2009**, *113*, 13266.
(14) Hayes, R.; Abedin, S. Z. E.; Atkin, R. *J. Phys. Chem. B* **2009**, *113*, 7049.
(15) Mezger, M.; Schramm, S.; Schroder, H.; Reichert, H.; Deutsch, M.; de Souza, E. J.; Okasinski, J. S.; Ocko, B. M.; Honkimaki, V.; Dosch, H. *J. Chem. Phys.* **2009**, *131*, 094701.
(16) Sha, M.; Zhang, F.; Wu, G.; Fang, H.; Wang, C.; Chen, S.; Zhang, Y.; Hu, J. *J. Chem. Phys.* **2008**, *128*, 134504.
(17) Rivera-Rubero, S.; Baldelli, S. *J. Phys. Chem. B* **2004**, *108*, 15133.
(18) Yoda, E. *J. Phys. Chem. C* **2009**, *113*, 9851.
(19) Schroder, U.; Wadhawan, J. D.; Compton, R. G.; Marken, F.; Suarez, P. A. Z.; Consorti, C. S.; de Souza, R. F.; Dupont, J. *New J. Chem.* **2000**, *24*, 1009.
(20) Lopes, J. N. A. C.; Padua, A. A. H. *J. Phys. Chem. B* **2006**, *110*, 3330.
(21) Wang, Y.; Voth, G. A. *J. Phys. Chem. B* **2006**, *110*, 18601.
(22) Xiao, D.; Hines, L. G.; Li, S.; Bartsch, R. A.; Quitevis, E. L.; Russina, O.; Triolo, A. *J. Phys. Chem. B* **2009**, *113*, 6426.
(23) Koddermann, T.; Wertz, C.; Heintz, A.; Ludwig, R. *Angew. Chem., Int. Ed.* **2006**, *45*, 3697.
(24) Sarkar, S.; Pramanik, R.; Ghatak, C.; Setua, P.; Sarkar, N. *J. Phys. Chem. B* **2010**, *114*, 2779.
(25) Attri, P.; Reddy, P. M.; Venkatesu, P.; Kumar, A.; Hofman, T. *J. Phys. Chem. B* **2010**, *114*, 6126.
(26) Trivedi, S.; Malek, N. I.; Behera, K.; Pandey, S. *J. Phys. Chem. B* **2010**, *114*, 8118.
(27) Chang, H. C.; Jiang, J. C.; Chang, C. Y.; Su, J. C.; Hung, C. H.; Liou, Y. C.; Lin, S. H. *J. Phys. Chem. B* **2008**, *112*, 4351.
(28) Chang, H. C.; Jiang, J. C.; Liou, Y. C.; Hung, C. H.; Lai, T. Y.; Lin, S. H. *J. Chem. Phys.* **2008**, *129*, 044506.
(29) Jiang, J. C.; Lin, K. H.; Li, S. C.; Shih, P. M.; Hung, K. C.; Lin, S. H.; Chang, H. C. *J. Chem. Phys.* **2011**, *134*, 044506.
(30) Jiang, J. C.; Li, S. C.; Shih, P. M.; Hung, T. C.; Chang, S. C.; Lin, S. H.; Chang, H. C. *J. Phys. Chem. B* **2011**, *115*, 883.
(31) Umebayashi, Y.; Jiang, J. C.; Shan, Y. L.; Lin, K. H.; Fujii, K.; Seki, S.; Ishiguro, S.; Lin, S. H.; Chang, H. C. *J. Chem. Phys.* **2009**, *130*, 124503.
(32) Scheiner, S.; Kar, T.; Pattanayak, J. *J. Am. Chem. Soc.* **2002**, *124*, 13257.
(33) Gu, Y. L.; Kar, T.; Scheiner, S. *J. Am. Chem. Soc.* **1999**, *121*, 9411.
(34) Masunov, A.; Dannenberg, J. J.; Contreras, R. W. *J. Phys. Chem. A* **2001**, *105*, 4737.
(35) Li, X.; Liu, L.; Schlegel, H. B. *J. Am. Chem. Soc.* **2002**, *124*, 9639.
(36) Hermansson, K. *J. Phys. Chem. A* **2002**, *106*, 4695.
(37) Jablonski, M.; Sadlej, A. J. *Chem. Phys. Lett.* **2008**, *463*, 322.
(38) Wong, P. T. T.; Moffatt, D. J.; Baudais, F. L. *Appl. Spectrosc.* **1985**, *39*, 733.
(39) Wong, P. T. T.; Moffatt, D. J. *Appl. Spectrosc.* **1987**, *41*, 1070.
(40) Koddermann, T.; Wertz, C.; Heintz, A.; Ludwig, R. *ChemPhysChem* **2006**, *7*, 1944.